Low-cost compact MEMS scanning LADAR system for robotic applications

Robert Moss, Ping Yuan, Xiaogang Bai, Emilio Quesada, and Rengarajan Sudharsanan
Spectrolab Inc., 12500, Gladstone Avenue, Sylmar CA 91342

Barry L. Stann, John F. Dammann, Mark M. Giza, William B. Lawler
Army Research Laboratory, 2800 Powder Mill Rd., Adelphi, MD, USA 20783-1138

ABSTRACT

Future robots and autonomous vehicles require compact low-cost Laser Detection and Ranging (LADAR) systems for autonomous navigation. Army Research Laboratory (ARL) had recently demonstrated a brass-board short-range eye-safe MEMS scanning LADAR system for robotic applications. Boeing Spectrolab is doing a tech-transfer (CRADA) of this system and has built a compact MEMS scanning LADAR system with additional improvements in receiver sensitivity, laser system, and data processing system. Improved system sensitivity, low-cost, miniaturization, and low power consumption are the main goals for the commercialization of this LADAR system. The receiver sensitivity has been improved by 2x using large-area InGaAs PIN detectors with low-noise amplifiers. The FPGA code has been updated to extend the range to 50 meters and detect up to 3 targets per pixel. Range accuracy has been improved through the implementation of an optical T-Zero input line. A compact commercially available erbium fiber laser operating at 1550 nm wavelength is used as a transmitter, thus reducing the size of the LADAR system considerably from the ARL brass-board system. The computer interface has been consolidated to allow image data and configuration data (configuration settings and system status) to pass through a single Ethernet port. In this presentation we will discuss the system architecture and future improvements to receiver sensitivity using avalanche photodiodes.

Keywords: ladar, lidar, laser radar, three-dimensional imaging, ground robots

1 INTRODUCTION

1.1. Prior Work

This paper builds on previous work done at Army Research Lab[1] (ARL) in which a brassboard ladar system was demonstrated and tested on an iRobot PackBot as well as under additional outdoor driving conditions in cluttered environments. ARL successfully built a breadboard ladar based on newly developed but commercially available components upon which Spectrolab is continuing to develop and take the next step towards a commercial product. The ARL ladar breadboard had a 5-6 Hz frame rate, an image size of 256 (h) x 128 (v) pixels, a 60º x 30º field of regard, 20 m range, eye-safe operation, and 40 cm range resolution. ARL also developed 3D visualization software and Ethernet software which allow image data to be captured and displayed by a computer running Windows. This is also currently being leveraged in current development and commercialization work.

1.2. Description of the Compact LADAR Imaging System

Boeing Spectrolab's fully functional prototype LADAR imaging system is shown in figure 1. The camera box dimensions are 3.5x6x11 inches with a weight 5.8 lb. The power consumption is 30 Watts and is passively cooled.

Laser Radar Technology and Applications XVII, edited by Monte D. Turner, Gary W. Kamerman,
Proc. of SPIE Vol. 8379, 837903 · © 2012 SPIE · CCC code: 0277-786X/12/$18 · doi: 10.1117/12.919804

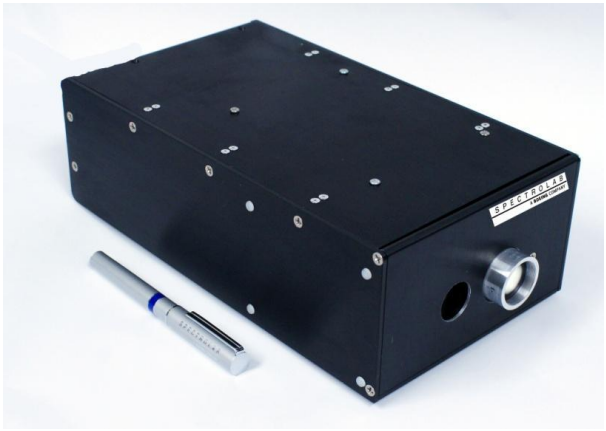

Figure 1. Spectrolab's Prototype LADAR Imaging System

Figure 3 shows the block diagram of the LADAR System. The ladar transmits a short optical pulse as a means to determine range to a target area and a two-axis MEMS mirror to establish the angular direction. Referring to figure 3, a trigger signal generated by the FPGA commands an erbium fiber laser to emit a short 2-3 ns pulse of light at a rate of 200 kHz that is collimated and then directed to the surface of a small 1.2 mm diameter MEMS mirror. Electrostatic actuators driven by a high voltage is used to tilt the mirror +/- 6.6º in the X axis and +/-3.3º in the Y axis (26.4º and 13.2º optical angle respectively peak-to-peak). The drive voltages are derived from values stored in the mirror memory flash, which are sent to a digital-to-analog converter (DAC) and high-voltage amplifier card set that interfaces to the FPGA. Light reflected from the mirror then passes through a telescope comprised of a convex lens followed by a concave lens that optically "amplifies" the scan angle of the MEMS mirror by 2.5 times. Light backscattered from the target is collected on the large face of a tapered fiber bundle that effectively increases the light capture area of the photo detectors; thereby, improving the SNR while maintaining a wide field-of-view. Photocurrents from four individual InGaAs PIN detectors are fed into monolithic 50-ohm microwave amplifiers, whose outputs are then combined to increase the SNR by a factor of two. The combined output is then split into low and high gain channels. The low and high gain channel outputs are then sent to differential amplifiers that are matched to the high speed ADC. The ADCs have 8-bit resolution and sample at a 1.5 giga-samples-per-second (GSPS) rate. A first-in first-out register (FIFO) on a field programmable gate array (FPGA) is used to buffer ADC data upon transmission of the laser pulse. The FPGA stores the amplitude and range data as a function of time from the ADC, determines the range to the pixel, and formats the image frames for transmission via Ethernet for display at a 5 Hz frame rate. A sample image capture is show in figure 2.

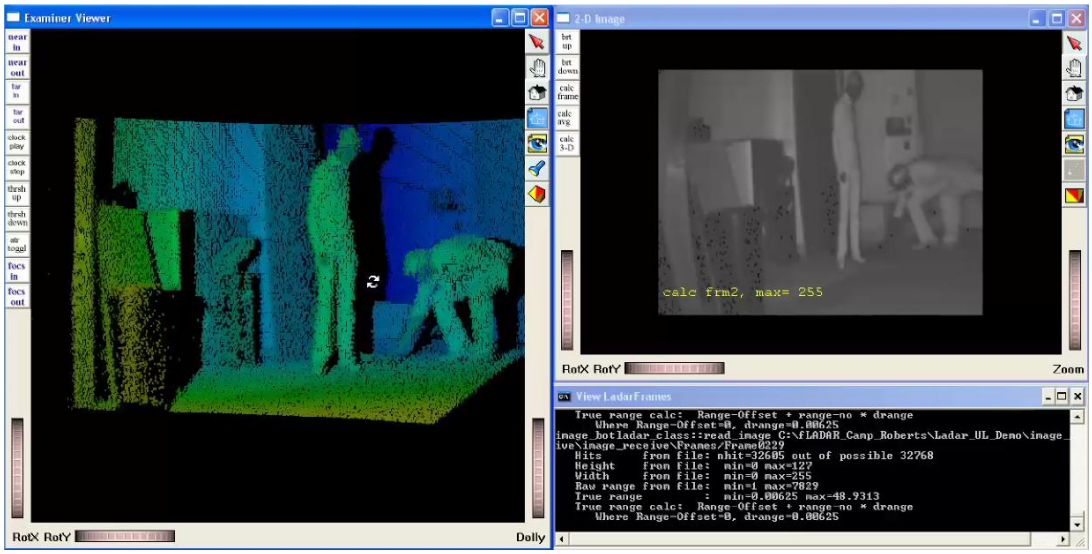

Figure 2. Sample Ladar Image data with the false color image on the left, the black and white (amplitude) image on the right and a window with frame and pixel range readout information below

The Ethernet board provides the interface between FPGA and external computer system by combining the frame data into Ethernet packets and streaming them via UDP protocol. Image frames are stored on the PC's hard drive as binary files, with each file composed of 256(H) x 128(V) pixels at 4 bytes per pixel, (2 bytes range + 2 bytes amplitude) resulting in a size of 128k bytes per frame. The Ethernet data throughput is 128k bytes per frame at 5 frames/second giving 640k bytes/second, or 5 Megabits per second (Mbps). The current 100 Mbps Ethernet system has excess bandwidth to support future increases in data rate. Each pixel is tagged with two 16-bit words, amplitude (first) and range (second). Only 13 least significant bits of the range word are used and only 10 bits of the amplitude word are used. The first two words of each frame are overwritten by a delimiter, FEDC BA98 (hex), placed so as to indicate the beginning of each frame. The next two words of each frame are overwritten with a frame count. Therefore, the first two pixels of the first line are non-image data. The new Ethernet board also accepts incoming Ethernet commands from an external host computer and passes them along serially to the FPGA for execution. The clock block of figure 3 is composed of a 60 MHz crystal which feeds a 1.5 GHz synthesizer that provides the master clock for both ADC and FPGA.

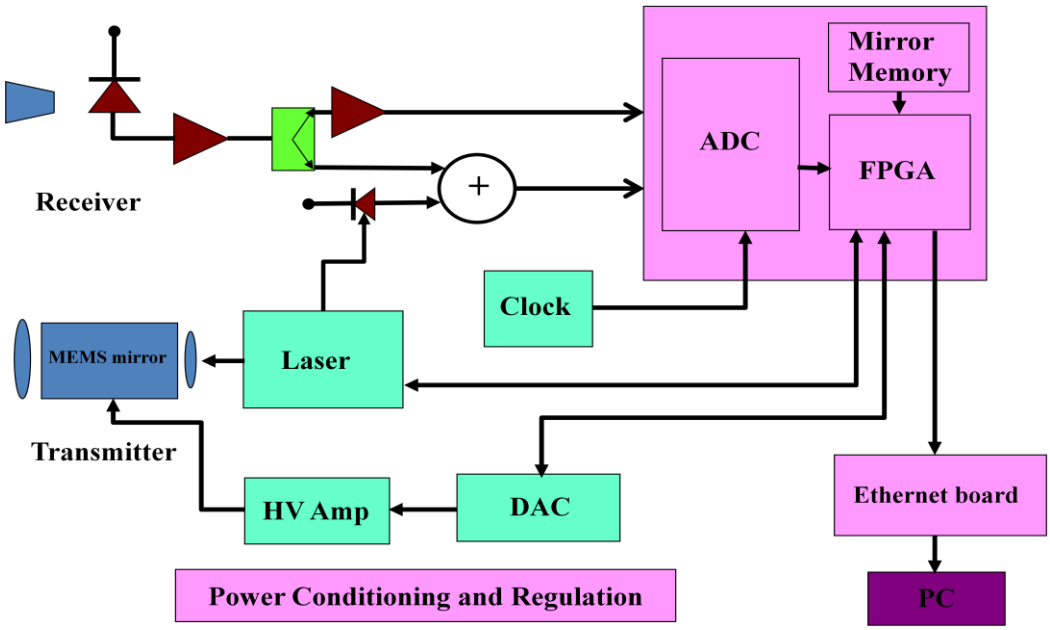

Figure 3. LADAR Imaging System Diagram

1.3. Specifications and Goals

The performance specifications are shown in figure 4. Boeing Spectrolab adopted these target specifications, in place since the beginning of ARL's research, were put in place in order to produce a ladar imager consistent with the needs of small military ground robots required to perform various tasks such as room clearing, remote ordinance identification, hazard removal, and room mapping. These key specifications have been met and demonstrated by ARL and recently by Spectrolab's prototype camera. The major specifications include 5 Hz frame rate, 20 m range, and 60° by 30° field of view. The theoretical designed field of view of 60° was not met due to optical attenuation caused by the receiver fiber taper at large input angles. We believe that the theoretical value can only be reached if the output of the fiber taper contacts the detectors. With the detectors used in the receiver, the bond wires are connected at the outer periphery of the detector and rise-up about 10 thousandths of an inch from the detector surface. To prevent damage to the bond wires, the output of the fiber taper is kept just above them. Future plans include using a backside illuminated detector which would

be flip-chip mounted and provide additional long-pass optical filtering for noise reduction. In the remaining gap, an index-matching fluid may be used between the detector and the fiber taper to reduce losses. The right hand part of the chart in figure 4 shows improvements in performance that can be made with little effort. The existing FPGA and Ethernet bandwidth is sufficient to double the frame rate from 5 Hz to 10 Hz; the laser pulse repetition frequency (PRF) can be increased from 200 KHz to 400 KHz to support the higher pixel rate.

Existing Performance	Easily Obtainable Performance
• 5-6 Hz frame-rate	• 10-12 Hz frame-rate
• 256 (h) x 128 (v) pixels	• 256 (h) x 128 (v) pixels
• 40° x 30° FOR	• 50° x 30° FOR
• 20 m range	• 40 m range
• 45 cm range resolution	• 45 cm range resolution
• 10 cm sample spacing	• 10 cm sample spacing
• 6.25 mm accuracy with range interpolation	• 6.25 mm accuracy with range interpolation
• Range and amplitude data	• Range and amplitude data
• 5 lb, 30 W power draw (24V, 1.25A)	• 3.5 lb, 18 W power draw (24V, 0.75A)

Figure 4. LADAR Imaging System Specifications

2 ADVANCES IN THE MEMS LADAR SYSTEM

2.1. Third Generation LADAR Receiver

In previous papers[1] we discussed the development of a second generation ladar receiver based on a tapered fiber bundle, a large area InGaAs PIN detector, and a low-noise microwave amplifier IC (MMIC). We use the large area detector and the tapered fiber bundle to capture more light over a wide field of view than possible with classical lens approaches thus increasing the SNR. The detector photocurrent is fed directly into the amplifier. This technique will lead to a receiver bandwidth too narrow to pass the 3 ns laser pulse because of the large capacitance of the detector. To increase the bandwidth of the receiver we placed a unique feedback circuit between the output and input of the amplifier, comprised of a series resistor, capacitor, and inductor. Although this second generation receiver served well, we explored improving its signal-to-noise ratio (SNR) by using another low-cost MMIC with a lower noise figure (.8 db) and a larger diameter detector. A breadboard using these components showed that the SNR could be increased. As a result, we planned to build a third generation receiver that would incorporate these and other improvements to simplify the receiver, and to provide built-in protective functions for the high-speed analog-to-digital converter (ADC). The new receiver eliminates the need for a large board between the receiver and ADC that previously performed these functions.

A block diagram of the third generation receiver is shown in figure 5. As in the second generation receiver, the four photocurrent amplifiers are configured with the same feedback circuit comprised of an inductor, capacitor, and resistor. The outputs of each amplifier feed a four-way microwave power combiner to effectively raise the SNR of the receiver two-fold. A lowpass filter follows the combiner to reduce any broadband noise beyond the bandwidth needed to pass the received laser pulses. The filtered signal then splits into a high gain and a low gain channel. This is done to equally share the dynamic range of the return pulses (72 dB) over the effective dynamic range of the two 8-bit ADCs (48 dB for one) in the ADC/FPGA board. The values of the attenuators in both the high and low gain channels are selected to allow linear collection of pulse amplitude data over the full dynamic range of the return pulses. Outputs from both channels are fed into the input of two differential amplifiers. These amplifiers are designed to clip hard at levels below those that may damage the subsequent ADCs. They also allowed dc connection to the ADCs, thereby reducing parts count and eliminating a stage of low frequency roll-off. Because the pulse returns from a target are mostly unidirectional, we

supply an offset bias to the differential amplifier inputs with current sources so that in the absence of signal, the ADCs will output digital numbers near zero. This offset allows us to use nearly all the dynamic range of the ADCs.

The third generation receiver circuit board was designed to accommodate detector chips up to 2 mm in diameter, the low noise amplifiers, differential amplifiers, and the other components as shown in the block diagram. The new layout shortens bond wires and lead lengths between the detector and the amplifier, and employs other practices common to good microwave layout. This new board confirmed that the SNR improvements are achievable with the 1.5 mm diameter detectors and low noise amplifiers. As mentioned the new receiver performs the filtering, gain adjustment, and limiting functions previously performed by the RF interface board (4" X 4"), thus eliminating the RF Board from the ladar system.

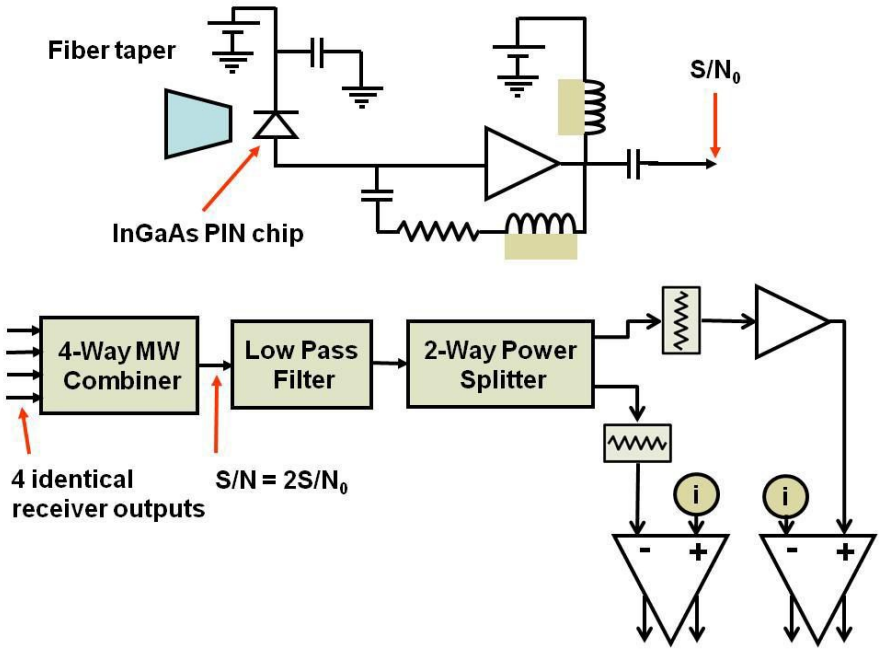

Figure 5. Third generation receiver block diagram.

Figure 6 shows an oblique and front view of the third generation receiver. Some of the key circuitry parts are indicated on the photos. The frontal dimensions of the receiver are 2.9" X 1.775".

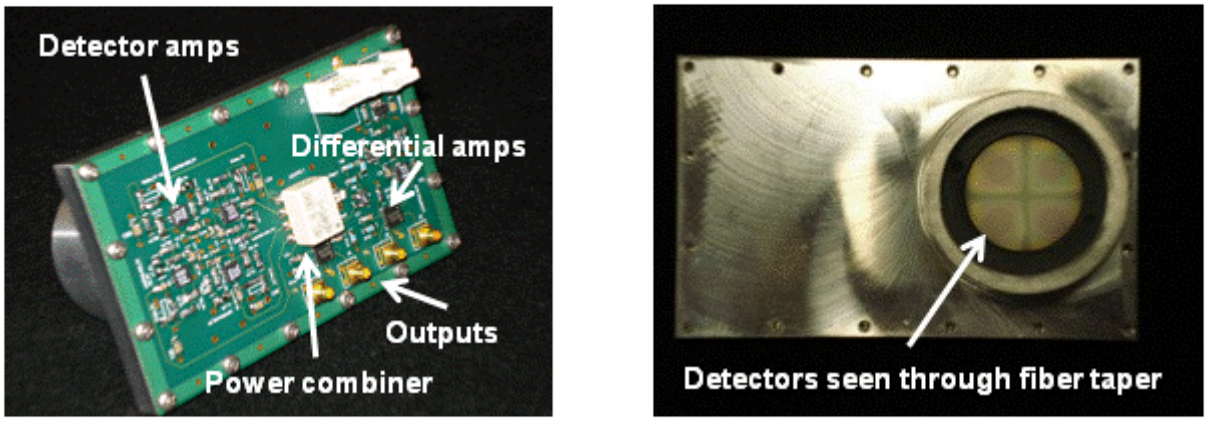

Figure 6. Oblique and front view of the third generation receiver.

The band-pass of the receiver was carefully measured using a source comprised of a low-power laser and a Mach-Zender E-O modulator. The Mach-Zender modulator was driven by a standard bench microwave signal generator. The high frequency -3 dB cut-off is 224 MHz and the low frequency cut-off is approximately 1.4 MHz. The signal amplitude is relatively flat from 30 MHz to the high frequency cut-off, but rises about 30 percent above the nominal level over the frequencies from 3 MHz to 25 MHz.

Figure 7 is the response of the receiver to the laser pulse as measured at the two outputs of the high-gain differential amplifier. The half-power (half-amplitude) points of the pulse are just under 3 ns. It is unclear how much stretching of the laser pulse occurs because the data sheet for the laser does not include the pulse width for this particular unit. A second purchased unit has had a measured pulse width of 2.6 ns; thus, it can most likely be concluded that some stretching is occurring.

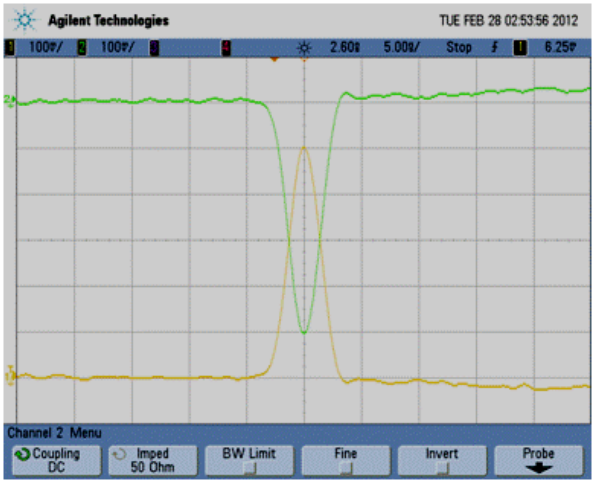

Figure 7. Pulse response of the third generation receiver showing the differential signals as they are arrive at the high-speed ADC inputs.

The receiver presently requires about 0.64 A at 3.3 volts minimum or 2.1 W. Further work will include testing another version of the low-noise amplifier which uses 50 ma less current per device or 0.25 Amps for the five used in the receiver; this would lower the total power to about 1.28 W. Calculations show that use of the lower power amplifier is feasible because in the worst case, the solar background signal will still only use about 10 percent of the available dynamic range of the amplifier.

The sensitivity of the receiver has not yet been measured to any high degree of accuracy. However, we know from the experience of operating the ladar breadboard both indoors and outdoors, that most scene materials are visible at ranges to about 30 m. This result is reasonably consistent with a simple model of the ladar written using MATLAB. For reference, the observed noise level of the receiver high gain channel when digitized and displayed as a function of time is contained mostly within the range of plus and minus 1-bit thus leaving most of the 8-bit ADC available for linear signal capture.

Over the past few months, both minor and substantial changes to the receiver have been found which could further improve the SNR. This improvement in SNR can be leveraged to either lower the laser power or increase the range. For example, the lowpass filter placed just after the 4-way combiner cuts off (-3 dB) at 460 MHz. This filter could be exchanged for one that cuts off at 230 MHz, thus removing about half the noise power from the received signal. If the pulse return is not significantly altered, this could raise the SNR by a factor of 1.4. Some minor SNR improvement could be achieved by installing a low loss solar filter with band-pass in the low 100's of nm. Further, the fiber taper should have coatings matched to the 1550 nm laser wavelength. This may increase the SNR by several percent. Some electromagnetic fields in the lab are picked up through the open design of the receiver box. A metal shield covering the exposed circuitry at the back of the receiver may suppress these fields and reduce noise. We have noticed some places in the printed circuit board layout where better microwave design practices are needed. If we perform a new layout of the board, we will also add circuitry and inputs to enable injection of the outgoing pulse into the data record as a means to better estimate target range.

The present receiver mostly meets the requirements of the original ground robot application; however, to expand the range of applications the SNR should be improved. To achieve this, new receiver designs may include modern commercial trans-impedance amplifiers. Though past experiments have shown commercial trans-impedance amplifiers to work no better than standard 50 ohm microwave amplifiers, revisiting the use of them may be worthwhile.
We may also use large area commercial avalanche photo detectors in place of the large area PIN detectors.

2.1. MEMS Mirror with Position Feedback

The transmitted laser beam is dynamically steered in a tip/tilt fashion by reflecting off the MEMS mirror surface. In the current design, the MEMS mirror is driven in an open-loop fashion whereby a data table of predefined mirror angles stored in flash memory is used to drive a high voltage amplifier which then directly drives the mirror. The mirror scan pattern is shown graphically in figure 8. The mirror angles (used by the FPGA to reconstruct the image) are based on commanded angle instead of actual mirror angle. This leads to pointing errors that will show up as image distortion as well as scrambled frames during a shock/vibe event.

Working with the MEMS Mirror vendor, Mirrorcle Technologies, a project has been initiated to incorporate an optical position sensor within the MEMS mirror package as well as a closed-loop proportional–integral–derivative (PID) control board. The closed-loop control board will use the error between the position feedback from the MEMS mirror and the FPGA's commanded position signal to drive the mirror with a corrected high voltage to dynamically compensate for pointing errors. Implementation of the mirror position feedback will allow the image processor to know if pixel angles aren't where they are commanded to be, and discard them if necessary while saving the validity of the frame. Having mirror position feedback will also make it possible to easily fulfill the laser safety requirement that the laser should be shut-off if the mirror stops scanning or changes substantially.

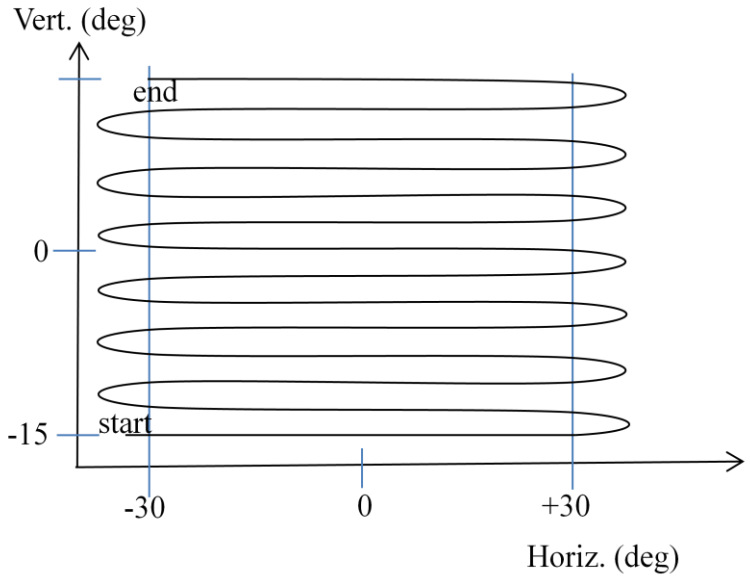

Figure 8. MEMS mirror scan pattern of a single frame. The scan begins in the bottom left of the scene as seen by someone behind the camera looking in the direction of an outgoing laser pulse. After the scan completes at the top left corner, the mirror jumps back to the starting position and the scan is repeated.

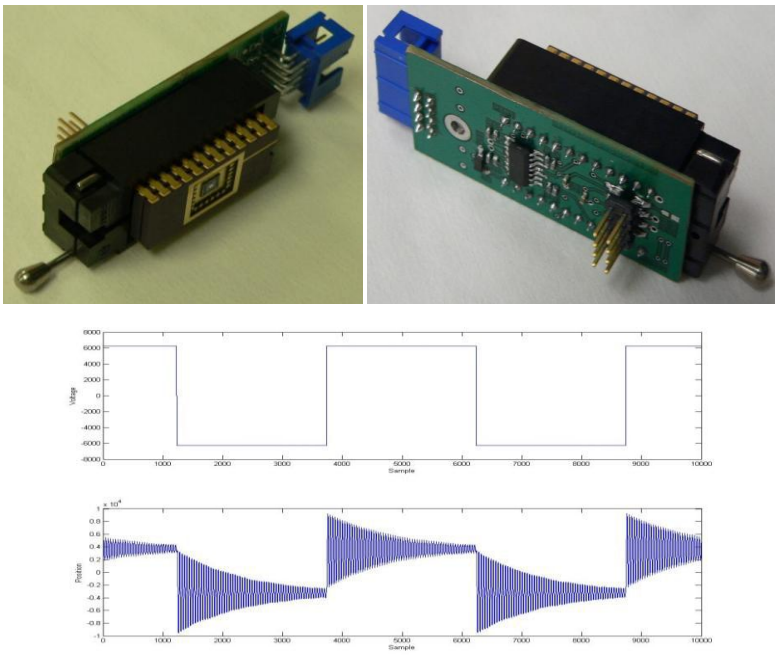

Figure 9. MEMS mirror with optical position sensor prototype unit and position signal resulting from being driven open-loop by a square wave input.

2.1. Enhanced Ethernet Interface Board

We have upgraded the capability of the Ethernet Interface board by adding the ability to handle bi-directional data and act as an interface to the FPGA's configuration commands. The previous Ethernet board could only stream UDP Ethernet data out; therefore, the system still required the use of an additional serial line connected to the ADC_FPGA board to control the LADAR system settings. With the new enhanced Ethernet Interface board, the Ethernet data is moving in both directions and is able to decode the Ethernet packets coming from the computer which are destined for the ADC_FPGA board. This has eliminated the need for a USB to Serial SPI converter that was being used to configure the LADAR system.

2.1. Optical T_0 Line

Current work is in progress to implement and optical "T_0" line, coming from the optical tap from the laser to a photodiode on the receiver, which will provide a direct indication of the time that each laser pulse was transmitted. Referring to system diagram in Figure 3, the low power optical tap is detected by a photodiode and electronically added to the receiver's low gain channel. The FPGA firmware then uses this pulse, the first one it detects on the low gain channel, as the time at which the pulse was transmitted. The current firmware assumes zero delay between pulse trigger sent to the laser, thereby relying on a user variable set by viewing the image data, which acts as a programmable delay. Implementation of the T_0 signal will provide better range accuracy and less range noise

2.2. User Friendly 3D Visualization Software

To support further productization, Spectrolab is developing a user-friendly software package that will combine the Ethernet package receive functionality and the 3D visualization functionality into a single Windows software package that will also provide an interface to the LADAR configuration command set.

3 FUTURE DEVELOPMENT

We feel that the current configuration of the LADAR camera system, with some minor improvements, is a commercially viable product. Moving forward to the next version, we feel that shrinking the LADAR camera package to less than half its current size is easily attainable. The current system has 11 pc boards. The next generation LADAR camera may contain only 5 pc boards with the ADC/FPGA board and Ethernet board combined into one main processor board. This board will also house the MEMS driver circuitry and Clock/Synthesizer Board. The Power Supply Board, Receiver and MEMS Mirrors will be the remaining boards. These changes will significantly reduce size, weight and cost of the current system. Continuing to improve the range capability, we plan to build a low-noise avalanche photo-diode (APD) based receiver which would give an order of magnitude better sensitivity. Using an APD-based receiver design, we expect to be able to image targets at 50 meters range with 0.1 reflectivity. Product development toward commercialization will include efforts to decrease laser power and increase receiver sensitivity while shrinking package size and power consumption. The current FPGA firmware has the ability to detect any of 3 return pulses: first, best or last. Returning all 3 pulses would increase the data throughput by 3 times. This can be easily handled by the current hardware and would only require a change in the image receive software located on the PC.

4 CONCLUSIONS

Spectrolab and ARL have successfully worked together to build and demonstrate a compact and portable LADAR imager that is equivalent ARL's brassboard system. This joint effort resulted in a camera that is being used to prove the commercial viability of the product. We plan to continue to work together to make design improvements. Spectrolab's work will continue on shrinking and ruggedizing the camera box while obtaining laser safety certification and MIL-STD-810E certification. The design focus of the LADAR camera product, as it evolves, will be pushing the range to beyond 50 meters, increasing the resolution past 256x128, increasing the receiver sensitivity (lower NEP), and lowering the laser transmitter power.

5 REFERENCES

[1] Stann, B. L. et. al., "Brass board development of a MEMS-scanned ladar sensor for small ground robots," *Proc. SPIE Laser Radar Technology and Applications XVI*, Vol. 8037, (2011).